Distribution of Halothane in a Dipalmitoylphosphatidylcholine Bilayer from Molecular Dynamics Calculations

Laure Koubi,* Mounir Tarek,*† Michael L. Klein,* and Daphna Scharf*‡

*Center for Molecular Modeling, Department of Chemistry, University of Pennsylvania, Philadelphia, Pennsylvania 19104-6323; †NIST Center for Neutron Research, National Institute of Standards and Technology, Gaithersburg, Maryland 20899-8562; and ‡Department of Anesthesia, Medical Center, University of Pennsylvania, Philadelphia, Pennsylvania 19104-4283 USA

ABSTRACT We report a 2-ns constant pressure molecular dynamics simulation of halothane, at a mol fraction of 50%, in the hydrated liquid crystal bilayer phase of dipalmitoylphosphatidylcholine. Halothane molecules are found to preferentially segregate to the upper part of the lipid acyl chains, with a maximum probability near the C_5 methylene groups. However, a finite probability is also observed along the tail region and across the methyl trough. Over 95% of the halothane molecules are located below the lipid carbonyl carbons, in agreement with photolabeling experiments. Halothane induces lateral expansion and a concomitant contraction in the bilayer thickness. A decrease in the acyl chain segment order parameters, S_{CD}, for the tail portion, and a slight increase for the upper portion compared to neat bilayers, are in agreement with several NMR studies on related systems. The decrease in S_{CD} is attributed to a larger accessible volume per lipid in the tail region. Significant changes in the electric properties of the lipid bilayer result from the structural changes, which include a shift and broadening of the choline headgroup dipole (P-N) orientation distribution. Our findings reconcile apparent controversial conclusions from experiments on diverse lipid systems.

INTRODUCTION

The effects of inhaled (volatile) anesthetics (IAs) on models of lipid membranes and in vivo have been extensively studied for over a century now with the goal to understand the mechanism of general anesthesia (Koehler et al., 1980; Franks and Lieb, 1982, 1994; Miller, 1985; Trudell, 1991; Curatola et al., 1991). Information on IAs partitioning between gas/lipid or into olive oil supported the experimental search for the site of anesthetic action in the lipid membrane. The results obtained by previous experimental studies (Kaneshina et al., 1981; Lieb et al., 1982; Tsai et al., 1987; Craig et al., 1987; Yokono et al., 1989) are difficult to examine critically because diverse lipids and different anesthetics at varying concentrations have been used. The location of anesthetics at clinical concentrations and their effects on the lipid structure are not well defined. Complementary experimental studies in the last 20 years or so shifted the focus from the lipids to direct binding to proteins (Franks and Lieb, 1984). More recently, it was suggested that the action of IAs may involve function modulation of a number of transmembrane ligand-gated ion channels (Curatola et al., 1991; Mihic et al., 1997; Eckenhoff and Johansson, 1997). Indeed, despite an overwhelming body of experiments, the controversy as to whether the IA primary site(s) of action is the membrane lipid or membrane proteins remains unresolved, rendering the mechanism for anesthetic action still unknown.

Most recently, renewed interest in the role of membrane lipids was ignited by a hypothesis regarding modifications in membrane structure induced by the presence of IAs, which in turn may indirectly alter membrane protein function (Cantor, 1997a, b; 1999). Additionally, a number of recent experimental studies on relatively simple model lipid systems continue the ongoing controversy as to the distribution of sites occupied by IAs in membranes. These include the acyl chain domain (Eckenhoff, 1996), various locations in the headgroup region (Baber et al., 1995; North and Cafiso, 1997), and the water/lipid interface (Trudell and Hubble, 1976; Xu and Tang, 1997; Tang et al., 1997).

Lieb et al. (1982) investigated the effect of halothane and chloroform at low concentration on the dimyristoylphosphatidylcholine (DMPC) lipid bilayer using Raman spectroscopy. They found that the anesthetic molecules induce no change on the lipid hydrocarbon chain conformations. Craig et al. (1987), using the same technique, detected only a small effect on the dipalmitoylphosphatidylcholine (DPPC) chain structure due to the presence of halothane. Both studies suggested that anesthetic molecules are likely located in the lipid headgroup region. Similar conclusions have been drawn from infrared spectroscopy results on DMPC for halothane, isoflurane, and chloroform (Tsai et al., 1987). Tang et al. (1997), using ^{19}F-NMR on halogenated compounds, inferred that anesthetic molecules distribute preferentially to regions of the membrane that permit easy contact with water. At high concentration, the interaction between methoxyflurane and DPPC vesicles was analyzed by nuclear Overhauser effect (NOE) difference spectroscopy (Yokono et al., 1989). It was deduced that the anesthetic resides preferentially at the membrane/water in-

Received for publication 15 June 1999 and in final form 10 November 1999.

Address reprint requests to Dr. M. L. Klein, Center for Molecular Modeling, Dept. of Chemistry, University of Pennsylvania, Philadelphia, PA 19104-6232. Tel.: 215-898-8571; Fax: 215-898-8296; E-mail: klein@lrsm.upenn.edu.

0006-3495/00/02/800/12 $2.00

terface. For halothane in DPPC vesicles, Tsai et al. (1990) found significant change in the stretching frequencies associated with the headgroup moieties. Both studies concluded again that the site of action is the headgroup.

In contrast to these studies, recent deuterium NMR and NOE measurements (Baber et al., 1995) on halothane, isoflurane, and enflurane in the palmitoyloleoylphosphatidylcholine (POPC) lipid bilayers at concentrations higher than 18 mol % suggest that the anesthetics are located primarily in the hydrocarbon chain region with only a slight preference for the membrane solution interface. Similar conclusions were also reported in NMR studies of the partially halogenated cyclobutane in POPC (North and Cafiso, 1997). The authors claim that the anesthetics are not found within the charged headgroup region.

Simulation of the free energy profiles (Pohorille et al., 1996) for methanol and ethanol in a simple lipid model support the water/lipid interface as the probable site for these two alcohols. The diversity of chemical properties, in particular relative hydrophobicity and molecular dipole moment, suggests that potent IAs like halothane could assume a distribution in a lipid membrane distinct from that of simple alcohols (Pohorille and Wilson, 1996).

We have used as a model lipid DPPC, which undergoes a phase transition to the biorelevant liquid crystalline phase (L_α) at temperatures above $T = 42°C$. A comprehensive description of the hydrated L_α phase of DPPC at $T = 50°C$, which accounts for all the known experimental properties, has been advanced by Tu et al. (1995). In a previous molecular dynamics (MD) simulation (Tu et al., 1998), we focused on the influence of halothane on this model bilayer at low concentration (6.5 mol %), which is directly relevant to clinical applications. In agreement with experiments, our results suggest that there is no detectable change in the overall lipid bilayer structure. Furthermore, although halothane molecules exhibited neither specific binding to the lipid headgroups nor specific orientation with respect to the lipid/water interface, there was fair agreement with several spectroscopic experimental studies. However, the low concentration of halothane (4 molecules in the 64 lipid system) precluded a thorough investigation of anesthetic distribution in the bilayer, which requires intensive statistical sampling. From the point of view of statistical mechanics, one of various strategies could have been adopted to improve the statistics to obtain a reliable probability distribution of IAs. One could have performed a large number of sufficiently long simulations at low concentration of IAs using multiple uncorrelated initial conditions. Alternatively, one could study an order of magnitude larger size system with a low (clinical) concentration of anesthetics for equal length of a simulation trajectory. Both these options entail computer resources well beyond what is currently affordable or available. Although this situation is likely to change, for the present we have chosen to study a larger number of anesthetic molecules in a relatively small bilayer, thus achieving enhanced statistics for a fixed amount of CPU resource. An examination of the above-mentioned experimental studies reveals that many have also been conducted with high concentrations of anesthetics for essentially the same reasons. Clearly, as in the present case, this is done at a risk of introducing modifications that may not be directly relevant to clinically applicable conditions.

Herein we report the results of a MD simulation of halothane in the DPPC bilayer at a lipid/anesthetic ratio of 2:1 (a mol fraction of 50%). The elevated concentration of anesthetic, compared with clinical application, has enabled us to efficiently sample the halothane distribution and determine its effect on the membrane structure. In this approach we follow in the footsteps of experiments at progressively higher anesthetic concentrations in attempting to infer the distribution of IAs at clinical level and changes in the lipid properties (Baber et al., 1995; North and Cafiso, 1997). As far as one can deduce from the available experimental data, higher concentrations of anesthetics in the range we consider here appear only to accentuate the physical phenomena observed at lower concentrations.

In the following sections we will briefly describe the simulation methodology. Results on the distribution of the anesthetic in the lipid will be presented and compared to experimental findings. The structural properties of the bilayer will be analyzed and compared to those of the pure lipid (Tu et al., 1995) and to our previous MD study at low anesthetic concentration (Tu et al., 1998).

METHODS

All inter and intramolecular interactions have been explicitly included in our simulations. We have used the parameter sets developed by Tu et al. (1995) for hydrated DPPC. It accounts, to within experimental error, for most of the measured properties of both the gel phase and the L_α phase of DPPC. For halothane we used the parameters developed by Scharf and Laasonen (1996) and the SPCE force field for water (Berendsen et al., 1987). Standard combination rules were applied for the cross-interactions among the lipid, the anesthetics, and water. Thus, the force field and potential parameters used in this study are similar to those we employed (Tu et al., 1998) in the earlier study of a clinical concentration (6.5 mol %) of halothane in the L_α phase of DPPC. The initial configuration of the bilayer consisted of 64 DPPC lipid molecules and 1792 water molecules in the biorelevant L_α phase. It was taken from the simulation of Tu et al. (1995). In this study 32 halothane molecules were initially uniformly distributed in the bilayer (see Fig. 1 *a*). The lipid region (-20 Å $< Z <$ $+20$ Å) was divided into eight equal volume segments. In each segment four halothane molecules were placed. No halothane was placed initially in the water region to account for the large experimental lipid-to-water partition coefficient of halothane (Kita et al., 1981; Roth and Miller, 1986; Franks and Lieb, 1990). To start the simulation, the halothane molecules were treated as point masses with zero charge and van der Waals parameters. Then, the halothane molecules were "grown" progressively. The details of this procedure are explained in our previous paper (Tu et al., 1998). The equilibration of the system was conducted first at constant volume and constant temperature, $T = 50°C$, (NVT) for 200 ps. This was followed by a 2-ns constant pressure, $p = 1$ atm, and temperature, $T = 50°C$, simulation (NPT) using the hybrid MD algorithm developed by Martyna et al. (1992, 1994). Averaged quantities were calculated over the

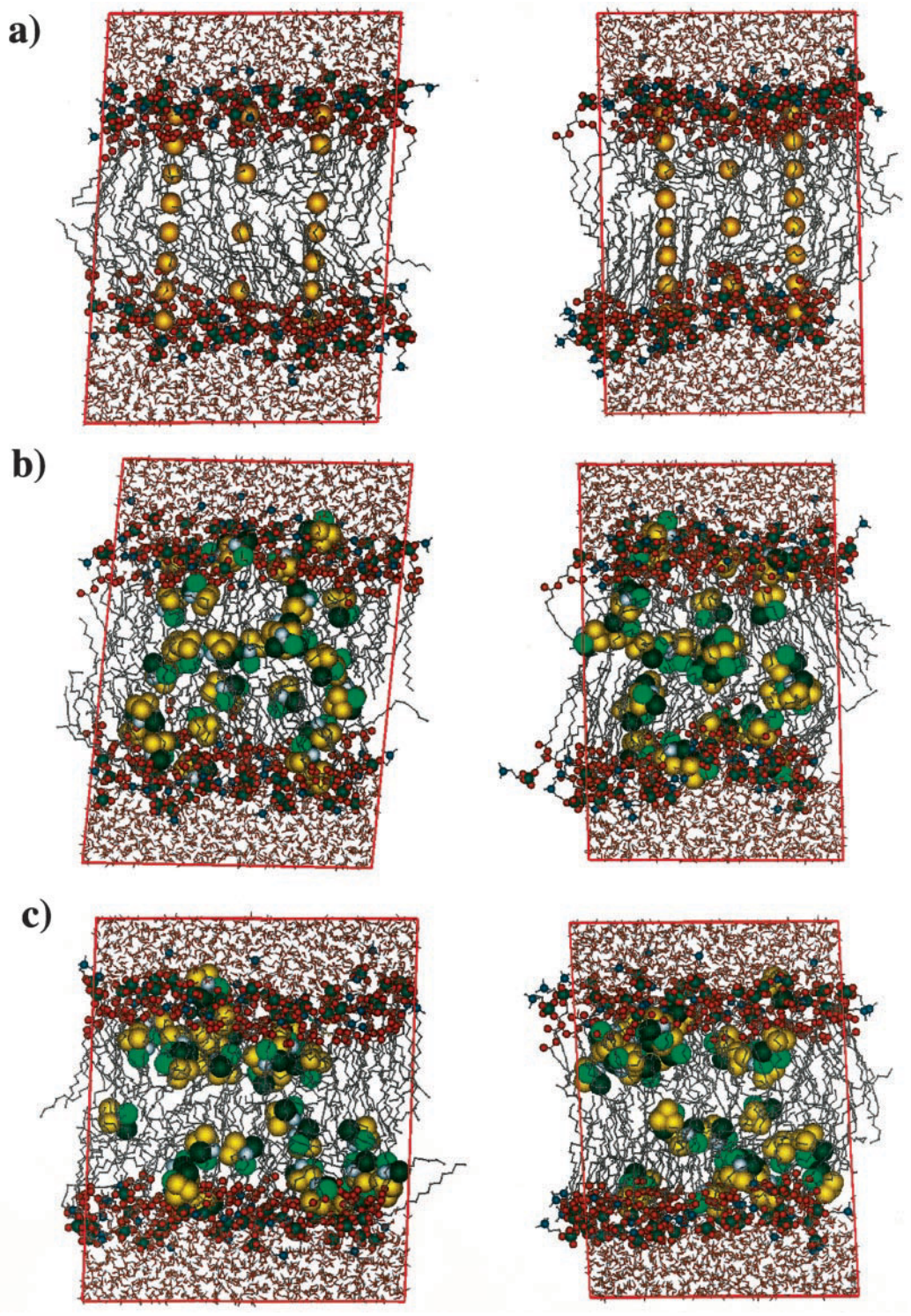

FIGURE 1 Panels of two orthogonal views, (XZ) and (*YZ*), of instantaneous configurations taken from the MD simulation. (*a*) Initial setup; (*b*) after 200 ps NVT run; (*c*) after 0.7 ns NPT run; (*d*) after 1.4 ns NPT run; (*e*) final configuration after 2 ns of NPT run. In (*a*), the yellow-orange spheres indicate the location of the halothane molecule centers of mass. In (*b*)–(*e*), halothane molecules are rendered with atomic van der Waals radii (F, *orange*; Cl, *light green*; Br, *dark green*; H, *gray*); the lipid acyl chains and the water molecules are shown in a ball-and-stick representation. The lipid P, N, and O atoms are displayed with covalent radii in green, blue, and red, respectively. Hydrogen atoms along the lipid acyl chains have been removed for clarity. The configurations (*a*)–(*e*) are all drawn on the same scale. Due to the periodic boundary condition the halothane molecule found in the water in (*d*) appears in the bottom of (*e*).

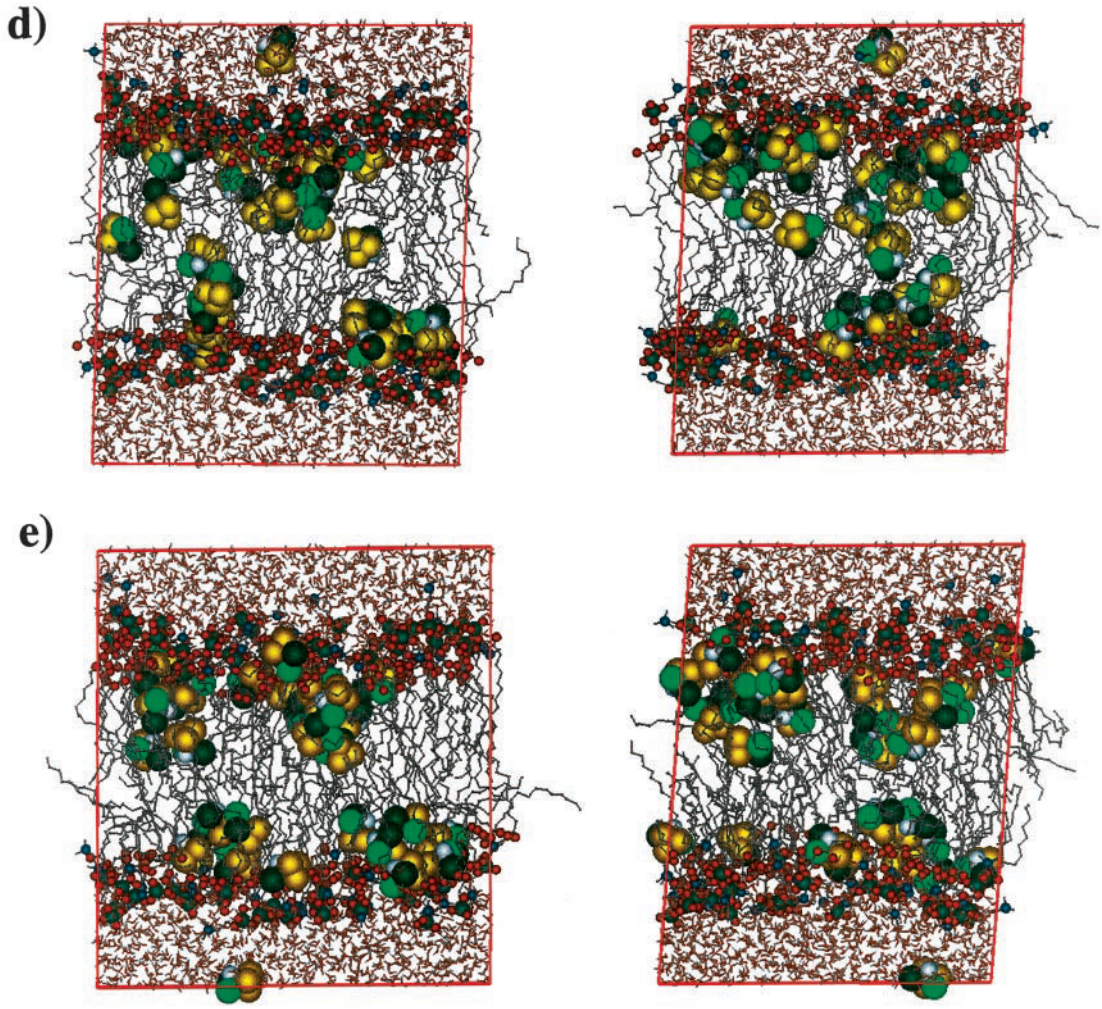

FIGURE 1 *Continued.*

last 1.5 ns of the NPT run. The calculations required 2.2 cpu h/ps, using 16 processors in a parallel/vector mode on the CRAY C90 computer at the Pittsburgh Supercomputing Center.

RESULTS AND DISCUSSION

Snapshots from the MD configurations are shown in Fig. 1 *a* for the initial setup, *b* after the 200-ps NVT run, and *c*--*e* after 0.7, 1.4, and 2 ns of the NPT run. Each panel shows two separate snapshots, which differ by a 90° rotation around the axis perpendicular to the bilayer surface (*Z* direction). Initially the anesthetic molecules are distributed more or less uniformly throughout the bilayer. This is also evident from the inset in Fig. 2, which shows the electron density distribution for halothane molecules along the *Z* direction. Already during the initial NVT equilibration there are noticeable changes in the halothane distribution, as is seen in Fig. 1 *b* and the inset in Fig. 2. Toward the end of the NPT run, the halothane molecules appear to have phase-segregated preferentially in the upper part of the lipid acyl chains, with fewer molecules found near the methyl trough region. Only a single halothane molecule migrated to the water region during the simulation (see Fig. 1, *d* and *e*). Segregation of IAs has been characterized experimentally only for anesthetic concentrations of 400 mol % (Gaillard et al., 1991). While noticeable in our study, it may not be detectable at low clinical concentrations.

The overall effect of the anesthetic presence at this concentration on the membrane structure is also visible in Fig. 1. The system contracts in the direction of the normal to the bilayer surface, whereas the bilayer area expands significantly. The calculated average area per lipid amounts to (72 ± 3.0) Å^2, compared to 61.8 Å^2 and 63.6 Å^2 for the L_α phase of the DPPC bilayer (Tu et al., 1995), and with low halothane concentration (Tu et al., 1998), respectively. This corresponds to an increase of ~16% compared with that of the pure lipid, and is in qualitative agreement with previous experiments and simulations of anesthetics in DMPC (Trudell, 1977; Lopez Cascales et al., 1998). Compared to

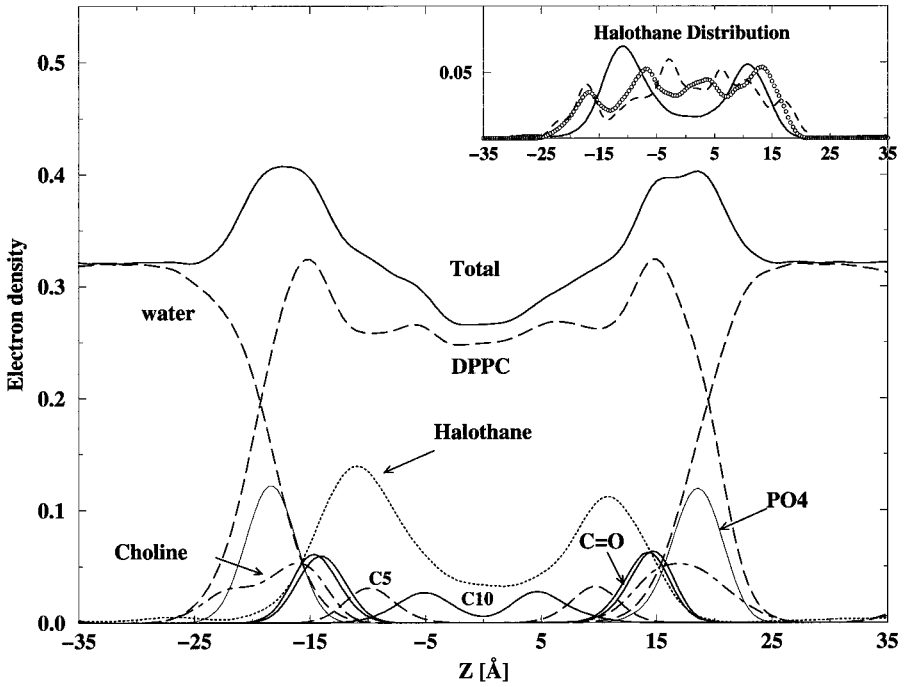

FIGURE 2 Electron density profiles along the bilayer normal, *Z*, averaged over the last 1.5 ns of the NPT trajectory. The contribution from the halothane molecules has been enhanced by a factor of 2 for clarity. *Inset:* initial halothane electron density distribution before (*circles*) and after NVT equilibration (*dashed line*) and final distribution (*solid line*).

the L_α phase of DPPC bilayers, the lamellar *d* spacing decreases ~8% from 67.3 Å (Tu et al., 1995) to (62 ± 3.0) Å. This is consistent with the 2% decrease found for the lower anesthetic concentration (Tu et al., 1998). The estimated total volume of the system increases to (141.0 ± 1.2) nm^3 compared to (134.1 ± 1.5) nm^3 and (134.6 ± 0.8) nm^3 for the neat DPPC and the low halothane concentration in DPPC, respectively. Using the experimental value for halothane molar volume measured in DPPC (Kita et al., 1981), the calculated volume expansion indicates that no additional free volume has been created due to the anesthetic presence to within computational error. This is in accord with our lower concentration study and with experimental results (Trudell, 1977; Franks and Lieb, 1981). Thus our findings contradict the proposed volume expansion mechanism (Kita et al., 1981).

In Fig. 2 we have plotted the average electron density profiles along the direction normal to the bilayer surface, *Z*, for the various lipid components and the halothane molecules. Averaging has been performed over the last 1.5 ns of the NPT run. Fig. 2 shows that the anesthetic molecules are located mainly along the lipid chains, below the carbonyl carbons. The anesthetic distribution is quite symmetric, with maxima around the C5 of the DPPC acyl chains, and flat finite minimum between the C10 and the C16, across the methyl trough (acyl chain nomenclature after Büldt et al., 1979). The resulting distribution is significantly different from the initial distribution, shown in the inset of Fig. 2. In equilibrium, on the average, over 94% of the anesthetic molecules reside below the carbonyl-carbon of the acyl chains. This is in excellent agreement with experimental results (Eckenhoff, 1996; Eckenhoff and Johansson, 1997). In an attempt to identify anesthetic binding domains on a ligand-gated ion channel, Eckenhoff et al. used halothane direct photoaffinity labeling of a nicotinic acetylcholine receptor in native Torpedo membranes. Thin-layer chromatograms showed that 94 ± 4% of label was localized below the carbonyls of the acyl chains for all the phospholipids studied, both saturated and unsaturated. This result is also consistent with experiments (Baber et al., 1995), which used ^1H-^1H NOE measurements between POPC and the halothane proton to demonstrate that the anesthetic molecules are not distributed at high concentration in the phospholipid headgroup region. The electron density distribution of the water molecules exhibit significant, finite overlap with the corresponding distributions for halothane and for the carbonyl carbons. From examination of radial distribution functions for water around each of the halothane molecules we have found that, on average, 50% of the halothane molecules are in contact with water for a significant time during the simulation, though not solvated as if they were immersed in bulk water. Such behavior has been demonstrated at low anesthetic concentration, and discussed in our previous study (Tu et. al., 1998). Fig. 2 shows that there is measurable anesthetic density in the methyl trough region. This also serves to demonstrate the significance of the migration dynamics exhibited by some of the halothane molecules. The trajectories of four of the halothane molecules along the bilayer normal *Z* are depicted in Fig. 3. Molecules (1) and (3) remained around their initial location. One molecule (2) is shown to have diffused from its original location to the bilayer center and cross the methyl trough

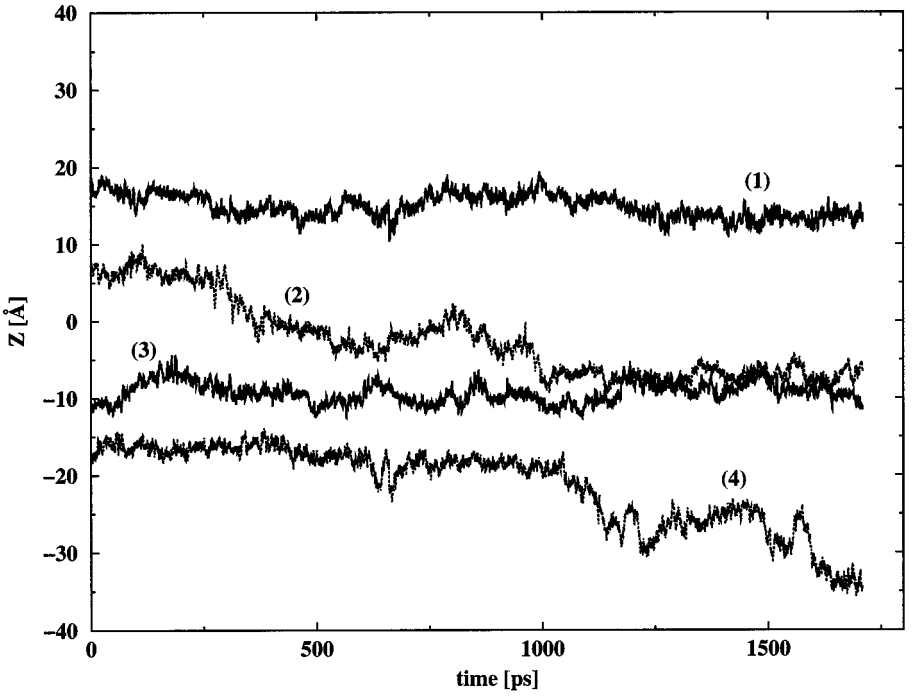

FIGURE 3 The center of mass position as a function of time for four of the halothane molecules projected onto the bilayer normal direction, *Z*.

region. We also noticed that molecule (4) migrated to the water region. This is the same molecule that is shown in Fig. 1, *d* and *e* residing in bulk water. The majority of the halothane molecules exhibit dynamics reminiscent of molecules (1) and (3), with gradual change in position along the bilayer normal, and small confined local dynamics in the *XY* plane of the bilayer.

The effect on lipid packing of small molecules, such as IAs distributing within membranes, can be experimentally deduced from changes in the segment C-D order parameter along the lipid chain (Boden et al., 1991). In deuterated lipids, the segment order parameter, $S_{mol} = \frac{1}{2}\langle 3\cos^2\theta - 1\rangle$, is used to characterize lipid conformations and can also be calculated (Seelig and Seelig, 1974). Here θ is the angle between the normal to the bilayer and the normal to the plane of the two C-D bonds in a deuterated methylene group of the lipid acyl chain. An S_{mol} value of 1 indicates that the chains are all *trans* and perpendicular to the bilayer plane, a value of -0.5 indicates that they are all *trans* and parallel to the plane, and 0 indicates random orientation. The experimental order parameter, S_{CD}, is derived from the measured residual quadrupole splitting $\Delta\nu = (\frac{3}{4})(e^2qQ/h)S_{CD}$ (Seelig and Seelig, 1974). Our MD simulations have been carried out with explicit hydrogens along the lipid chains and not for deuterated lipids. In the following calculated segment order parameters we assume that the configurations of the deuterated lipids are identical to those with explicit hydrogens. In classical MD simulation there is no difference in equilibrium distributions between H or D, unless the H/D substitution also results in changes in interatomic interactions. Fig. 4 *a* displays the averaged segment order parameters $S_{CD} = -\frac{1}{2}S_{mol}$ calculated from the MD trajectory for the DPPC lipid with and without halothane. Also shown, for comparison, are the order parameters from the low

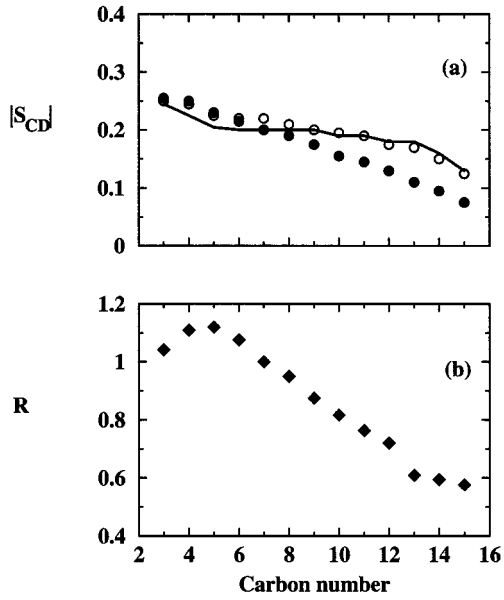

FIGURE 4 (*a*) Average deuterium acyl chain segment order parameters (S_{CD}) for halothane mol fraction of 50% (*solid circles*) compared with S_{CD} for the DPPC L_α phase (*line*), and for the low halothane concentration, 6.5 mol % (*open circles*). (*b*) Relative order parameters, *R*, as a function of the segment position for a mol fraction of 50% halothane. A value >1.0 indicates an increase, a value <1.0 indicates a decrease in the segment order parameter.

halothane concentration study (Tu et al., 1998). Although the latter results are very close to the pure lipid values, we notice that at high halothane concentration there is an increase in S_{CD} for the first few segments at the top of the acyl chains and a decrease below the C6 carbon. For comparison with experiments, Fig. 4 *b* displays the relative order parameter *R*, calculated from the ratio of the order parameters in the presence of given concentrations of halothane and the order parameter for the pure lipid bilayer. In agreement with NMR results (Baber et al., 1995; North and Cafiso, 1997), we find that for high anesthetic concentration $R > 1.0$ for the upper segments of the acyl chain and decreases significantly at the end of the acyl chain. To complement our study on the effects induced by the anesthetics on the hydrocarbon chain structure, we have also analyzed the chain defects. We present the percentage of *gauche* defects in the last 12 bonds of the hydrocarbon chain both for the high anesthetic concentration and for the pure lipid (Table 1). Even though the differences between the two systems are small, the present results indicate that the acyl chains have more *gauche* rotamers toward the middle of the chain compared to the case of pure lipids.

Our analysis is in agreement with the direct NMR and relative order parameter measurements of Baber et al. (1995) and North and Cafiso (1997), but offers an alternative explanation and picture to parts of their interpretation. Here, we have shown that the anesthetic molecules are primarily distributed in the upper portion of the acyl chain, below the carbonyl carbons. The decrease in the order parameters along the lipid chains for lipid segments below the C6 results from the increased mobility of the lipid tails in the plane of the lipid bilayer, which now has larger accessible area per headgroup. The lipid chains are dynamically more disordered, except for the region constrained by the concentrated physical presence of halothane, i.e., the upper part of the acyl chain.

To investigate the new organization of the lipid molecules, we show in Fig. 5 the electron density profile along the bilayer normal *Z*, averaged over the last 1.5 ns of the run. Fig. 5 *a* displays the overall density profile and the separate contributions from the DPPC and the water molecules. The electron density contributions from the polar groups, i.e., the choline group, the phosphate, and the acyl ester groups, are shown in Fig. 5, *b–d*, respectively. The results are compared with the profiles obtained for the low anesthetic concentration and for the pure DPPC liquid crystalline phase. At high anesthetic concentration, the overall profile peaks around −17.0 Å and +16.0 Å compared to −19.0 Å and + 8.8 Å for the pure DPPC. Franks and Lieb (1979) in their x-ray results, found that even in the presence of anesthetic at high concentration (up to 60 mol %), the membrane thickness is unchanged. Although our results are in apparent disagreement with their finding, the changes observed herein are likely to fall within the resolution of the x-ray data. Moreover, their experiment was performed for the gel phase, while our calculations are done for the L_α phase.

The thickness of the lipid membrane estimated from the distance between the peaks of the PO_4 distributions is 38.0 Å compared to 39.8 Å for the pure lipid. Only subtle changes are noted for the carbonyl carbon profile. The most noticeable change upon addition of halothane is in the choline groups distribution. At high anesthetic concentration, the corresponding electron density profile displays broad distributions, clearly shifted toward the interior of the bilayer (Fig. 5 *b*). The estimated peak-to-peak distance is now equal to 34 Å compared to 42 Å and 38 Å for the L_α pure lipid and for the low anesthetic concentration in it. Table 2 shows the distances from the bilayer center for some carbon atoms of the choline moiety/group and of the acyl chain. It further demonstrates that the methyl groups of the choline group are closer to the bilayer center at high halothane concentration compared with the pure DPPC. Fig. 6 shows the electron density profile for some carbon atoms of the acyl chain. From Fig. 6 combined with the data of Table 2 we deduce interdigitation of the lipid chains from the two leaflets of the bilayer at high anesthetic concentration.

To fully characterize the zwitterion headgroup conformation, we calculated the probability distribution of the P-N dipole with respect to the bilayer normal *Z* (see Fig. 7). In all the cases the P-N dipole orientation distribution is bimodal. However, for the pure lipid, a significant fraction of dipoles point at a small angle from the bilayer normal ($0° < \theta < 30°$) and there is an equally large population of molecules with dipole orientations in the range $80° < \theta < 120°$, i.e., flat with respect to the bilayer surface or even slightly oriented toward the interior of the bilayer. At low anesthetic concentration, the population of dipoles oriented toward the interior of the bilayer increases, whereas fewer P-N dipoles are within a small angle of the bilayer normal. At high anesthetic concentration, this trend is drastically accentuated and many of the lipid dipoles are on the average oriented toward the interior of layer ($\theta > 90°$).

TABLE 1 Average percentage of *gauche* defects in the last 12 bonds of the DPPC lipid hydrocarbon chains

Bond	C_3–C_4	...	...	C_6–C_7	...	...	C_9–C_{10}	...	...	C_{12}–C_{13}	...	C_{14}–C_{15}
L_α	14	25	18	23	20	20	20	23	23	25	26	32
High	15	22	24	23	22	25	23	26	26	27	28	32

Comparison between the pure lipid (L_α) and high anesthetic concentration (High). Standard deviations are typically 10%.

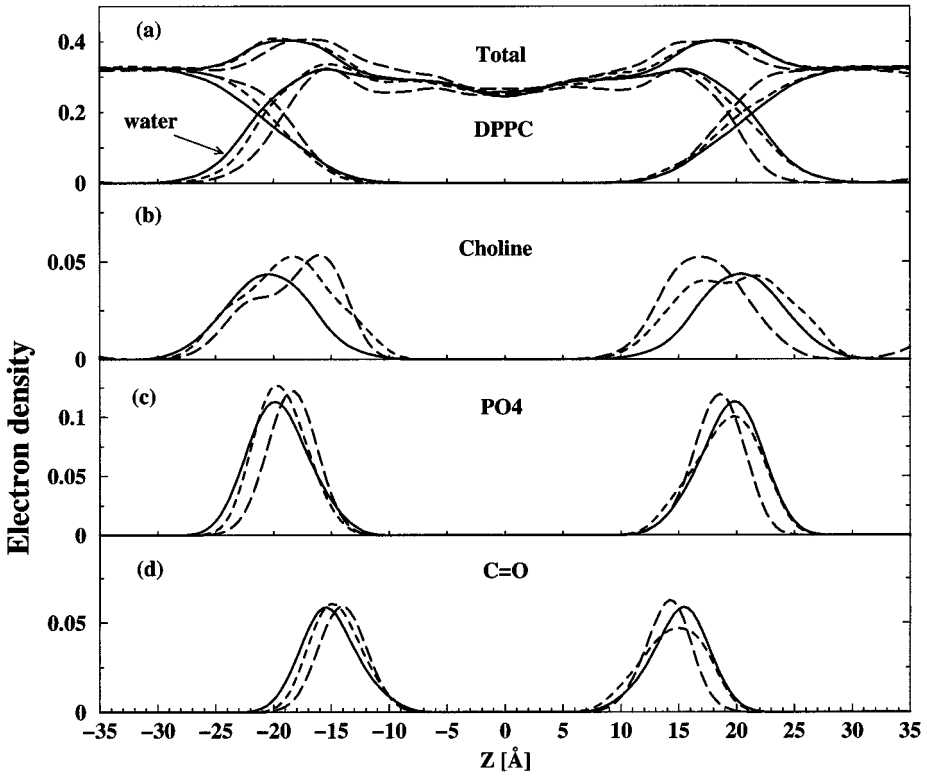

FIGURE 5 Selective electron density profiles for a mol fraction of 50% halothane in DPPC along the bilayer normal direction, *Z*, averaged over the last 1.5 ns of the NPT trajectory. (*a*) The overall profile, the water, and the pure DPPC contributions; (*b*) the choline $N(CH_3)_3$ contributions; (*c*) PO_4 contributions; (*d*) the C═O contributions averaged over the two distinct acyl chains. Shown are results for the neat L_α phase of DPPC (*solid lines*), plus halothane at mol fraction of 6.5% (*dashed lines*) and mol fraction of 50% (*long-dashed lines*).

This modification of the headgroup orientation in comparison to the neat L_α phase of DPPC is in agreement with the hypothesis of Gaillard et al. (1991). In their NMR study of halothane in DPPC they suggested that the decrease in chemical shift anisotropy could be due to a change in the average headgroup orientation with respect to the bilayer normal. An important consequence follows the reorientation of the lipid dipole: the choline group is now experiencing a different water environment. Indeed, integration of the water/nitrogen radial distribution functions amounts to 15.3 water molecules in the first hydration shell of the choline group compared with 17.3 water molecules for the pure lipid phase (Fig. 8 *a*). This indicates a moderate dehydration of the choline group. No significant modification is observed for the phosphate group first hydration shell, and only a very a small effect is apparent on the hydration of the two glycerol ester carbonyl carbon atoms C_{21} and C_{31} (Fig. 8, *b* and *c*).

This new P-N orientation distribution is also likely to affect the charge distribution along the direction of the bilayer normal, and in turn the measurable potential difference *V* across the lipid/water interface (Feller et al., 1996). We estimated *V* from the MD simulation as a double integral of molecular charge density distributions, neglecting the explicit electronic polarization, as suggested by Tobias et al. (1997) (Fig. 9). The potentials display a monotonic decrease through the bilayer/water interface to a value in the water of ~ -500 mV for neat DPPC, -920 mV for the low anesthetic concentration, and -880 mV for the high halothane concentration. In Fig. 9 *b* we present individual contributions from the DPPC and water molecules. Although the negative contribution in the phosphate region is almost completely offset for the pure DPPC, we notice that the addition of halothane molecules produces an overall negative contribution of >280 mV and 350 mV at low and high anesthetic concentration, respectively. The water potential decreases to -650 mV for the low anesthetic concentration, whereas no modification is observed at high concentration compared to the lipid in absence of halothane.

TABLE 2 Average distances (Å) of carbon atoms from the bilayer center

Atom	C_γ	C_β	C_α	C_{GC3}	C_5	C_9	C_{14}	C_{15}
L_α	20.2 (2.4)	20.3 (2.6)	21.1 (3.0)	17.2 (2.1)	10.7 (1.8)	6.9 (2.0)	2.6 (2.0)	1.9 (2.1)
Low	19.2 (2.6)	19.2 (3.3)	19.2 (4.0)	17.4 (1.7)	10.9 (2.2)	6.7 (2.3)	2.5 (3.6)	1.8 (3.6)
High	16.2 (4.0)	17.1 (3.2)	18.1 (3.0)	16.8 (2.2)	9.9 (2.5)	5.8 (2.7)	0.0 (3.6)	0.3 (3.6)

Comparison between pure lipid (L_α), low, and high anesthetic concentrations of the corresponding distances from the bilayer center to selected DPPC headgroup and acyl chain carbon atoms. For nomenclature see Büldt et al. (1979). Standard deviations are in parentheses.

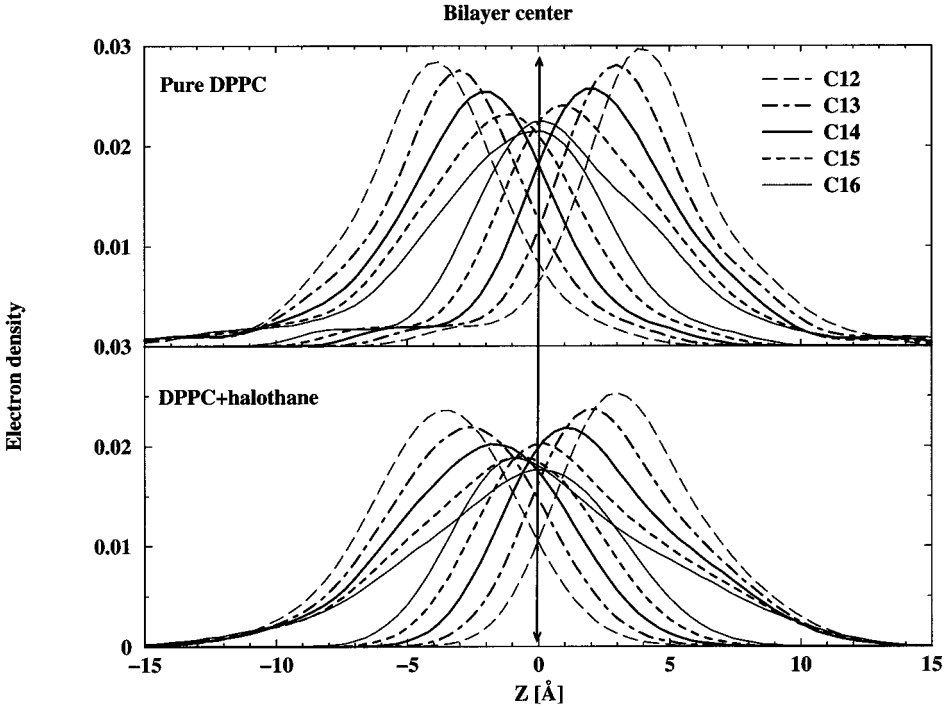

FIGURE 6 Electron density profiles along the bilayer normal, *Z*, for different carbon atoms of the lipid chains: (*a*) the neat L_α phase of DPPC and (*b*) DPPC with halothane at a mol fraction of 50%. For nomenclature see Büldt et al. (1979).

Using voltage-sensitive spin probes, Qin et al. (1995) found that anesthetic molecules induce a decrease in the membrane dipole potential. To understand these different results, it is important to notice that, first, Qin et al. (1995) used a different lipid and a different anesthetic concentration, factors that may influence the result. Second, here the values of the potential difference across the interface calculated from the MD simulations are only for the hydrated lipid component, and exclude the halothane contribution. Last, our results are somewhat dependent on the time length over which the average is performed. A more accurate estimate can be obtained only if the trajectory is long enough to permit a complete sampling of the headgroup motions, which are known to be in the range of tens of nanoseconds time scales (Pastor and Feller, 1996; Tobias et al., 1997; Feller and Pastor, 1997; Essmann and Berkowitz, 1999). However, the results presented here clearly indicate that the anesthetic certainly induces significant structural changes in the lipid that, in turn, most probably should lead to significant modification to the measured potential across the membrane. Changes in the potential across the membrane are known to influence membrane protein function. The modifications introduced by incorporating halothane in the DPPC bilayer suggest that membrane protein function could be altered indirectly by the presence of IAs in the membrane, in addition to a possible direct interaction with membrane proteins. We have chosen to study a relatively high concentration of anesthetic in a model bilayer primarily to obtain the distribution of halogenated anesthetics in a model lipid bilayer. We have found halothane to exhibit a nonuniform distribution along the acyl chain component of the model lipid bilayer. The simulation pertains to the correct biological phase relevant to physiological condi-

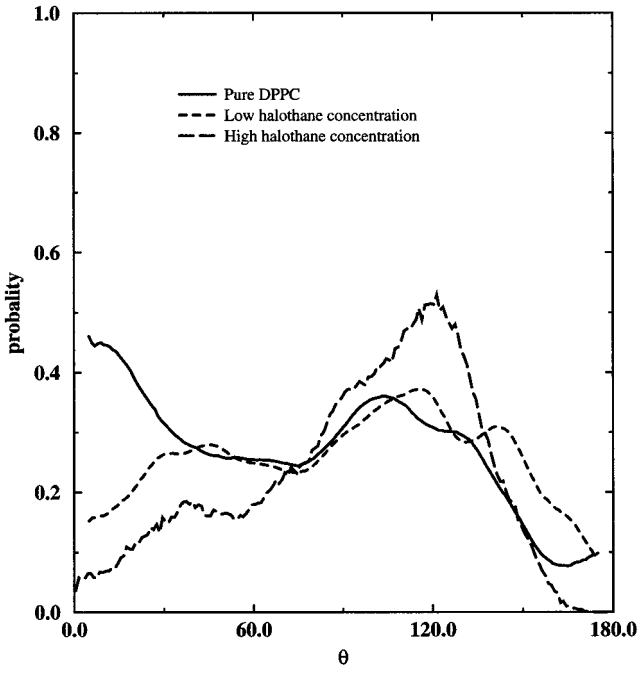

FIGURE 7 The orientation distribution of the lipid headgroup P-N dipole with respect to the bilayer normal direction, *Z*. The DPPC L_α phase is shown in a solid line, halothane mol fraction of 6.5% in a dashed line, and halothane mol fraction of 50% in a long-dashed line.

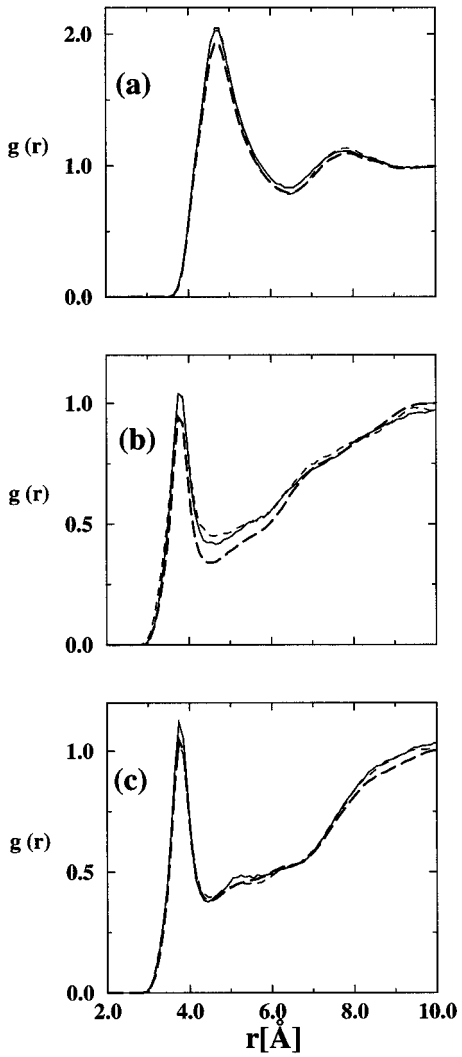

FIGURE 8 Radial distribution functions, $g(r)$, for the oxygen atom of the water molecules around the phospholipid headgroup and glycerol ester carbonyl carbon atoms (C_{21} and C_{31}), current study in long dashed lines, compared to data for the neat L_α phase of DPPC, solid lines, and to halothane mol fraction of 6.5%, dashed lines. (*a*) N of the choline, (*b*) C_{21} and (*c*) C_{31} atoms. Notice the difference in scale between (*a*) and the others.

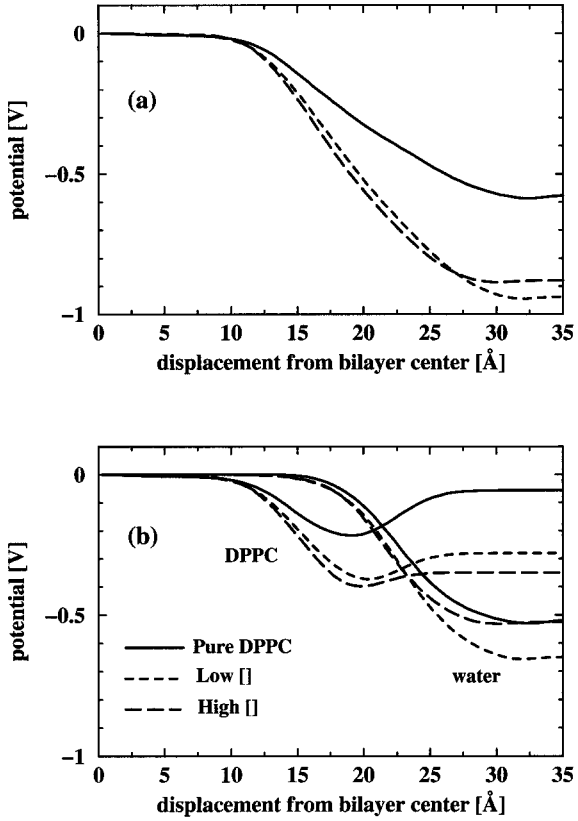

FIGURE 9 Electrostatic potential difference relative to the bilayer center computed from the simulations with 6.5 mol % halothane (*dashed line*), 50 mol % (*long-dashed line*), and neat L_α phase of DPPC (*solid line*): (*a*) total; (*b*) individual contributions from water and DPPC molecules.

tions. But, unfortunately, it was necessary to use a concentration much above the estimated clinical range.

CONCLUSIONS

The distribution of IAs in membrane is of seminal importance in the search for the sites and mode of IAs action. The known high partition coefficients for IAs into olive oil has long suggested that lipids play a significant role in anesthesia, either in mediating or as being the site where action is rendered. Our results shed a new light on theories and experiments targeted at the lipid component of membranes. Our main result of a nonuniform distribution of IAs along the membrane is a key assumption and a prerequisite in the theory of Cantor (1997a, b; 1999). Thus, our results offer some support to Cantor's hypothesis for IAs mechanism. A nonuniform distribution may have implications regarding the accessibility of various protein interfaces to anesthetic molecules partitioned into the membrane lipid component. It may influence the direct specific binding probability, if this mode of action proves to be at the core of anesthesia mechanism. Our results require further experimental verification, in particular studies performed at higher resolution and careful preparations. The calculated halothane distribution should be reexamined to determine possible changes and dependency on the choice of anesthetic and the exact anesthetic concentrations. For a given choice of anesthetic and concentration, additional simulations are required to determine the effect of single and multiple unsaturations in the lipid and the mixture of lipids that better model biological membranes. It is plausible that other IAs, e.g., ether derivatives and alcohols, exhibit different equilibrium distribution in lipid bilayers.

This study of halothane at 50 mol % in a model lipid bilayer demonstrates that this anesthetic distributes preferentially along the upper portion of the lipid acyl chain,

below the carbonyl carbon. The incorporation of halothane at this elevated concentration causes significant modifications of the bilayer structure. Most notable is the change in the orientation of the headgroup P-N dipole, besides an increase in the area per lipid headgroup along with contraction along the bilayer normal direction and a net change in volume, which is comparable to the volume of the added anesthetics. Our finding of increased acyl tail mobility, accompanied by an increase in the *gauche* rotamer defects, complements the calculated and experimentally measured trend for reduction in the acyl chain segment order parameter, S_{CD}, in the lower half of the lipid acyl chain. The preferred location of halothane in the upper half of the acyl chain explains the slight gain in S_{CD} due to physical restriction of the motion in the upper part of the lipid acyl chains. A number of additional predicted changes should be open to experimental verification: a tendency of the anesthetics to segregate, the change in hydration of the choline moiety, but not the phosphate, and a change in the orientation distribution of the lipid dipoles. Our calculated distribution of halothane in a model lipid bilayer combined with its dynamics confirms and reconciles diverse experimental results of NMR, NOE, x-ray, and photolabeling, some of which were in apparent disagreement. Although the nonuniform distribution of halothane observed in this simulation suggests support for the hypothesized indirect mechanism of anesthetic action (Cantor et al., 1997a, b; 1999), direct interaction with membrane proteins cannot be ruled out. The present results have been obtained for an anesthetic concentration well above clinically relevant ones. It remains an open question and a challenge to confirm whether the proposed distribution found here is exhibited at clinical concentrations.

We thank Profs. Roderic G. Eckenhoff, Douglas Tobias, and Dr. Kechuan Tu for helpful discussions.

This study was supported by National Institutes of Health Grant GM55876. Computer resources were provided by the Pittsburgh Supercomputer Center under grant CHE 980006P and National Partnership for Academic Computing Infrastructure under grant MCA93S020.

REFERENCES

Baber, J., J. F. Ellena, and D. S. Cafiso. 1995. Distribution of general anesthetics in phospholipid bilayers determined using ^{2}H-NMR and ^{1}H-^{1}H NOE spectroscopy. *Biochemistry.* 34:6533–6539.

Berendsen, H. J. C., J. R. Grigera, and T. P. Straatsma. 1987. The missing term in effective pair potentials. *J. Phys. Chem.* 91:6269–6271.

Boden, N., S. A. Jones, and F. Sixl. 1991. On the use of deuterium nuclear magnetic resonance as a probe of chain packing in lipid bilayers. *Biochemistry.* 30:2146–2155.

Büldt, G., H. U. Gally, J. Seelig, and G. Zaccai. 1979. Neutron diffraction studies on phosphatidylcholine model membranes. I. Head group conformation. *J. Mol. Biol.* 134:637–691.

Cantor, R. S. 1997a. The lateral pressure profile in membranes: a physical mechanism of general anesthesia. *Biochemistry.* 36:2339–2344.

Cantor, R. S. 1997b. Lateral pressure in cell membranes: a mechanism for modulation of protein function. Mechanism of general anesthesia. *J. Phys. Chem. B.* 101:1723–1725.

Cantor, R. S. 1999. Lipid composition and the lateral pressure profile in bilayers. *Biophys. J.* 76:2625–2639.

Craig, N. C., G. J. Bryant, and I. W. Levin. 1987. Effect of halothane on dipalmitoylphosphatidylcholine liposomes: a Raman spectroscopic study. *Biochemistry.* 26:2449–2458.

Curatola, C., G. Lenaz, and G. Zolese. 1991. *In* Drugs and Anesthetic Effects on Membrane Structure and Function. L. C. Abia, C. C. Curtain, and L. M.Gordon, editors. Wiley-Liss, New York. 35–70.

Eckenhoff, R. G. 1996. An inhalational anesthetic binding domain in the nicotinic acetylcholine receptor. *Proc. Natl. Acad. Sci. USA.* 93: 2807–2810.

Eckenhoff, R. G., and J. S. Johansson. 1997. Molecular interactions between inhaled anesthetics and proteins. *Pharmacol. Rev.* 49:343–367.

Essmann, U., and M. L. Berkowitz. 1999. Dynamical properties of phospholipid bilayers from computer simulation. *Biophys. J.* 76:2081–2089.

Feller, S. E., and R. W. Pastor. 1997. Length scales of lipid dynamics and molecular dynamics. *Pacific Symposium on Biocomputing '97. World Scientific.* 142–150.

Feller, S. E., R. W. Pastor, A. Rojnuckarin, S. Bogusz, and B. R. Brooks. 1996. Effect of electrostatic force truncation on interfacial and transport properties of water. *J. Phys. Chem.* 100:1701–1720.

Franks, N. P., and W. R. Lieb. 1979. The structure of lipid bilayers and the effects of general anesthetics. An x-ray and neutron diffraction study. *J. Mol. Biol.* 133:469–500.

Franks, N. P., and W. R. Lieb. 1981. Is membrane expansion relevant to anesthesia? *Nature.* 292:248–251.

Franks, N. P., and W. R. Lieb. 1982. Molecular mechanisms of general anesthesia. *Nature.* 300:487–493.

Franks, N. P., and W. R. Lieb. 1984. Do general anesthetics act by competitive binding to specific receptor? *Nature.* 310:599–601.

Franks, N. P., and W. R. Lieb. 1990. Mechanisms of general anesthesia. *Environmental Health Perspectives.* 87:199–205.

Franks, N. P., and W. R. Lieb. 1994. Molecular and cellular mechanisms of general anesthesia. *Nature.* 367:607–614.

Gaillard, S., J.-P. Renou, M. Bonnet, X. Vignon, and E. J. Dufourc. 1991. Halothane-induced membrane reorganization monitored by DSC, freeze fracture electron microscopy and P-NMR techniques. *Eur. Biophys. J.* 19:265–274.

Kaneshina, S., H. Kamaya, and I. Ueda. 1981. Transfer of anesthetics and alcohols into ionic surfactant micelles in relation to depression of Krafft-point and critical micelle concentration, and interfacial interaction of anesthetics. *J. Colloid. Interface Sci.* 83:589–598.

Kita, Y., L. J. Bennett, and K. W. Miller. 1981. The partial molar volumes of anesthetics in lipid bilayers. *Biochim. Biophys. Acta.* 647:130–139.

Koehler, L. S., E. T. Fossel, and K. A. Koehler. 1980. A multinuclear magnetic resonance study of the interaction of halothane and chloroform with phosphatidylcholine vesicles. *In* Molecular Mechanism of Anesthesia. E. Fink, editor. Raven Press, New York. 447–455.

Lieb, W. R., M. Kovalycsik, and R. Mendelsohn. 1982. Do clinical levels of general anesthetics affect lipid bilayers? Evidence from Raman scattering. *Biochim. Biophys. Acta.* 688:388–398.

Lopez Cascales, J. J., J. G. Hernandez Cifre, and J. Garcia de la Torre. 1998. Anesthetic mechanism on a model biological membrane: molecular dynamics simulation study. *J. Phys. Chem.* 102:625–631.

Martyna, G. L., M. L. Klein, and M. Tuckerman. 1992. Nosé-Hoover chains: the canonical ensemble via continuous dynamics. *J. Chem. Phys.* 97:2635–2643.

Martyna, G. J., D. J. Tobias, and M. L. Klein. 1994. Constant pressure molecular dynamics algorithms. *J. Chem. Phys.* 101:4177–4189.

Mihic, S. J., Q. Ye, M. J. Wick, V. V. Koltchine, M. D. Krasowski, S. E. Finn, M. P. Mascia, C. F. Valenzuela, K. K. Hanson, E. P. Greenblatt, R. A. Harris, and N. L. Harrison. 1997. Sites of alcohol and volatile anaesthetic action on GABA sub A and glycine receptors. *Nature.* 389:385–389.

Miller, K. W. 1985. The nature of the site of general anesthesia. *Int. Rev. Neurobiol.* 27:1–61.

North, C., and D. S. Cafiso. 1997. Contrasting membrane localization and behavior of halogenated cyclobutanes that follow or violate the Meyer-Overton hypothesis of general anesthetic potency. *Biophys. J.* 72: 1754–1761.

Pastor, R. W., and S. E. Feller. 1996. Time scale of lipid dynamics and molecular dynamics. *In* Biological Membranes: A Molecular Perspective from Computation and Experiment. K. M. Merz, Jr., and B. Roux, editors. Birkhauser, Boston. 3–29.

Pohorille, A. P., P. Cieplak, and M. A. Wilson. 1996. Interactions of anesthetics with the membrane-water interface. *Chem. Phys.* 204: 337–345.

Pohorille, A., and M. A. Wilson. 1996. Excess chemical potential of small solutes across water-membrane and water-hexane interface. *J. Chem. Phys.* 104:3760–3773.

Qin, Z., G. Szabo, and D. S. Cafiso. 1995. Anesthetics reduce the magnitude of the membrane dipole potential. Measurements in lipid vesicles using voltage-sensitive spin probes. *Biochemistry.* 34:5536–5543.

Roth, S. H., and K. W. Miller (Editors). 1986. Appendix. *In* Molecular and Cellular Mechanisms of Anesthetics. Plenum Publishing Corp., New York.

Scharf, D., and K. Laasonen. 1996. Structure, effective pair potential and properties of halothane. *Chem. Phys. Lett.* 258:276–282.

Seelig A., and J. Seeling. 1974. The dynamic structure of fatty acyl chains in a phospholipid bilayer measured by deuterium magnetic resonance. *Biochemistry.* 13:4839–4845.

Tang, P., B. Yan, and Y. Xu. 1997. Different distribution of fluorinated anesthetics and non-anesthetics in model membrane: an ^{19}F-NMR study. *Biophys. J.* 72:1676–1682.

Tobias, D. J., K. Tu, and M. L. Klein. 1997. Atomic-scale molecular dynamics simulations of lipid membranes. *Curr. Opin. Colloid Interface Sci.* 2:15–26.

Trudell, J. R. 1977. The membrane volume occupied by anesthetic molecules: a reinterpretation of the erythrocyte expansion data. *Biochim. Biophys. Acta.* 470:509–510.

Trudell, J. R. 1991. Role of membrane fluidity in anesthetic action. *In* Drugs and Anesthetic Effects on Membrane Structure and Function. L. C. Abia, C. C. Curtain, and L. M. Gordon, editors. Wiley-Liss, New York. 1–14.

Trudell, J. R., and W. L. Hubble. 1976. Localization of molecular halothane in phospholipid bilayer model nerve membranes. *Anesthesiology.* 44:202–205.

Tsai, Y. S., S. M. Ma, H. Kamaya, and I. Ueda. 1987. Fourier Transform Infrared Studies on the phospholipid hydration: phosphate-oriented hydrogen bonding and its attenuation by volatile anesthetics. *Mol. Pharmacol.* 26:603–606.

Tsai, Y. S., S. M. Ma, S. Nishimura, and I. Ueda. 1990. Infrared spectra of phospholipid membranes: interfacial dehydration by volatile anesthetics and phase transition. *Biochim. Biophys. Acta.* 1022:245–250.

Tu, K., M. Tarek, M. Klein, and D. Scharf. 1998. Effects of anesthetics on the structure of a phospholipid bilayer: molecular dynamics investigation of halothane in the hydrated liquid crystal phase of dipalmitoylphosphatidylcholine. *Biophys. J.* 75:2123–2134.

Tu, K., D. J. Tobias, and M. L. Klein. 1995. Constant pressure and temperature molecular dynamics simulation of a fully hydrated liquid crystal phase dipalmitoylphosphatidylcholine bilayer. *Biophys. J.* 69: 2558–2562.

Xu, Y., and P. Tang. 1997. Amphiphilic sites for general anesthetic action? Evidence from ^{129}Xe-^{1}H intermolecular nuclear Overhauser effects. *Biochim. Biophys. Acta-Biomembranes.* 1323:154–162.

Yokono, S., K. Ogli, S. Miura, and I. Ueda. 1989. 400 MHz two dimensional nuclear Overhauser spectroscopy on anesthetic interaction with lipid bilayer. *Biochim. Biophys. Acta.* 982:300–302.